Dense Water Overflows and Cascades

by H. C. Mansley

Supervised by Prof. D. Marshall

Declaration

I confirm that this is all my own work and that information obtained from other sources is appropriately acknowledged.

Abstract

This study reviews our current knowledge of the main physical processes affecting the dynamics and properties of dense water overflows and cascades in the ocean. Dense water formed by cooling, evaporation or sea-ice formation in the surface layer of the ocean descends into a deep ocean basin over sloping topography as an overflow or cascade. Large-scale overflows provide substantial contributions to globally important water masses that ventilate the abyssal ocean and force the global meridional overturning circulation. Our understanding of dense water overflows is far from comprehensive due a lack of observations and the complexity of their dynamics. Problems with resolution, mixing and bottom drag, and subsequent model dependence on simple parameterisations, lead to highly unrealistic representation of overflows in current ocean circulation and climate models.

Dense bottom flows descend under a balance of gravity,

Contents

Chapter 1

Introduction and Motivation

Very dense waters may be formed in the surface layer of the ocean through cooling, evaporation or sea ice formation over the continental shelf* or in a semi-enclosed or marginal sea [Condie, 1995]. The resulting horizontal density gradient drives an exchange flow between these dense waters and the open ocean [Ivanov et al., 2004]. The dense water enters a deep ocean E-0.00031 Tc -0.00031c0 Tc 0 Tw 0 Ts rw54.4599

The dense overflow descends to a depth where its density is equal to that of the ambient ocean water. This depth depends on its initial water mass properties and the entrainment and properties of surrounding water during its descent. The descended wate

still not fully understood. Research to understand and assess their contribution to deep water formation continues to be a major effort in oceanography.

The purpose of this study is to review our current knowledge of the main physical processes affecting the dynamics and properties of dense flows descending sloping topography. We begin in Chapter 2 with a brief discussion of the main processes contributing to dense water formation, the essential physical features of regions where this occurs, the contribution of observed overflows and cascades to abyssal water mass formation, and the main issues surrounding the inadequate representation of overflow dynamics in ocean models. In Chapter 3 we describe the balance of forces controlling the downslope propagation of the dense flow, and discuss the main processes affecting the density and volume properties of the overflow, the dependence of the product water on the properties of the source water, the ambient water, and the roles of entrainment and detrainment. A simple plume model is used in Chapter 4 to isolate and analyse the roles of bottom topography and friction in determining the path, the rate of descent, and the evolution of the thickness and width of the outflow. We conclude with a discussion of future work needed to improve our understanding of both dense overflow processes and climate.

2.2. Dense water formation

due to atmospheric forcing in shallow areas, where the water depth is less than the depth of penetrating convection, can create a nearly homogenous mass of cold or salty dense water [S

The resulting flows produce an irreversible exchange between ocean and shelf or sea waters [Shapiro et al., 2003]. In the Faroe Bank Channel outflow and the Medite

2.4. Observed overflows and cascades

Although dense water formation and outflows down steep topography are a widespread occurrence in the global oceans [Shapiro and Hill, 1997; Lane-Serff, 2001], not all may contribute to the ventilation of the abyssal ocean layers. Dense water produced over the continental shelf may be far from the open ocean and must propagate a large distance across the shelf before reaching the steep continental slope. Its transport over a gently sloping or flat bottom, such as that of the shelf, is generally quite slow and there may be a relatively long interval between dense water formation and the initiation of cascading [Shapiro and Hill, 1997]. On its path, the dense water will entrain considerable amounts of relatively light ambient shelf water before reaching the slope [Schauer and Fahrbach, 1999] and could partially lose its density excess. This may lead to weaker cascading or the dense flow not reaching the slope [Shapiro et al., 2003]. For example, dense water may be produced very effectively at sites such as near the Central Bank in the Barents Sea [Quadfasel et al., 1992], but may not ventilate the deep ocean since it loses its density excess during its several hundred kilometre journey toward the shelf edge. A comprehensive study by Ivanov et al. [

dense bottom flows outside the Weddell Sea could be thin, due to a lack of topographic constraints, and thus difficult to detect.

major sources of intermediate water entering the North Atlantic [Price, 1994]. A schematic of the abyssal circulation in the Atlantic forced by the principal overflows is shown in Figure 2.2.

Model results [e.g. Döscher and Redler, 1997] indicate that deep water form

circulation is sensitive to the dynamical details of large-scale overflows [e.g. Döscher and Redler, 1997; Willebrand et al. 2001], and it is certain that they are integral to the formation of important water masses.

Our understanding of dense water overflows is far from comprehensive, largely because of the difficulties associated with obtaining observations and the complexity of their dynamics. Importantly, the contribution of mesoscale cascades to dense water mass formation is unknown. Problems with resolution, mixing and bottom drag, and subsequent model dependence on simple parameterisations, lead to highly unrealistic representation of overflows in current ocean circulation and climate models. To remedy this we must first develop a physical understanding of the fundamental dynamical processes occurring in overflows. In the next chapter, we shall review current knowledge of the main processes affecting dense overflow dynamics.

Chapter 3

Dynamics of overflows: theories, experiments and observations

3.1. Introduction

Dense water cascading down sloping bathymetry is an extremely complex phenomenon involving numerous mesoscale processes and effects. Overflows and cascades are density driven and therefore any process that alters their density affects their evolution, in particular, the volume and tracer properties, the path taken and the final depth reached. We thus expect the dense plume to distort in a complex way over time because of local effects [Shapiro and Hill, 1997].

In this chapter, a combination of theories, observations and results from laboratory experiments and numerical models is used to provide a review our current knowledge of the main physical processes affecting the dynamics and properties of dense water outflows. We first describe the balance of forces controlling the downslope propagation of the dense flow and examine a variety of downslope transport mechanisms. We consider physical characteristics of the dense flow, the bathymetry, and the ambient water that can affect the force balance and discuss their main effects. The final product water that disperses into the ocean interior is very different from the source water before its descent. This is of particular importance to the depth reached by the overflow and its associated transports. We identify the main processes affecting the density and volume properties of the overflow. We further discuss the dependence of the product water on the properties of the source water and the ambient water, and the roles of entrainment and detrainment.

3.2. Forces controlling the flow

On the continental shelf, frictional forces are relatively small and in steady state conditions dense water flow over a relatively large horizontal scale (~10 km) is in geostrophic balance and horizontal along density fronts [Gill, 1982]. This tends to produce a front at or near the shelf break separating dense shelf water from lighter off shelf waters. However, dense

3.3.1. Friction

A dense bottom flow becomes more energetic on the steep continental slope due to gravitational acceleration [Ivanov et al., 2004]. Flow speeds can be 10-100 times faster than most other deep ocean flows [Lane-Serff, 2001] and friction is considerably increased in this region. In consequence, friction is

In addition, stratification of the ambient water increases the stretching parameters and increases eddy production. There are also indications that the eddy propagation speed along the slope is lessened by stratification, possibly due to internal wave generation [Lane-Serff, 2001].

Figure 3.1
Columns of fluid,9c7j10.9c3Figure 3.1

The relative importance of viscous effects is connected to the ratio of the boundary layer thickness to the thickness of the dense outflow. For an intense supply, the dense plume or sheet is thick (compared to the thickness of the Ekman layer) and therefore bottom friction effects are relatively unimportant to the motion of the plume [Baines and Condie, 1998; Shapiro and Hill, 1997].

For this reason, along slope flow is in approximate inviscid geostrophic balance over most of the depth of the layer, with externally imposed currents driving thick plumes in the direction of flow [Shapiro and Hill, 1997]. The dense fluid is still continuously drained at its base by the viscous bottom layer, which takes fluid from the base of the current at an angle down the slope [Lane-Serff, 2001]. However, water transports within the Ekman layer account for only a small portion of the total downslope transport [Baines and Condie, 1998; Shapiro and Hill, 1997] and the evolution of the near inviscid outflow is therefore mostly governed by geostrophy, and mixing [Condie, 1995].

In summary, an intense level of dense water production creates a thick broad plume or sheet on the continental slope in which eddies may form. The outflow is mostly governed by geostrophy and the long-term density driven evolution of the dense water on sloping topography is principally along slope. It is continuously drained in the Ekman layer and the outflow stretches from the source, in a sheet, plume or in a series of domes, mostly along depth contours and slightly down slope [e.g. Jungclaus and Backhaus, 1994] until it reaches the bottom, or its own density level. A schematic of this process is

correspondingly reduced. In a thinner layer, friction restricts the growth of baroclinic instabilities and thus eddy production [Condie, 1995; Lane-Serff and Baines, 1998]. Eddy transport provides a smaller component of the downslope motion than Ekman drainage. The descent of the plume or filament down sloping bathymetry is, however, predominantly geostrophic and most of the downslope transport is above the boundary lay

insights into the overflow process. Cascading is to a high degree related to geostrophic along-slope flow. In many overflows, the effect of the bottom friction is constrained to a bottom boundary layer and viscous down-slope motion is mostly confined to within this lower layer [Condie, 1995; Shapiro & Hill, 1997; Whitehead, 1993]. However, there are some strong turbulent overflows, such as the Mediterranean overflow in which properties are well mixed.

An intense source producing a thick broad plume fits well with the large-scale overflows from marginal seas, for example the Weddell Sea or through the Denmark Strait where the predominant balance is geostrophic and frictional effects are relatively small. Cascades, which tend to

pronounced in the cold outflow and its descent through the weakly stratified warmer ocean waters is dominated by the thermobaric effect [Killworth, 1977]. In the Mediterranean, the outflow water is warm and saline and the thermobaric effect is reversed, retarding the descent of the flow through colder oceanic waters. However, as already mentioned, the effect is relatively small in comparison to the effects of entrainment and stratification in these warm waters [Backhaus et al., 1997].

In an investigation of the thermobaric effect [Jungclaus et al., 1995] the downslope propagation of a cold plume may be retarded by the thermobaric effect. The enhanced dynamics of the modelled cold plume also increase

continental slope [J

example, the even more vigorous entrainment resulting from arbitrarily increasing the density of the model Mediterranean source water by 1 kg m^{-3} increases the transport of product water by about 10^6 m^3 s^{-1} and limits the increase in density of the product water to only about 0.15 kg m^{-3} [Price, 1994], indicating that entrainment is a crucial component of abyssal water production.

In addition, entrainment mixes substantial volumes of ambient water into the dense overflow. Quadfasel et al. (1988), for example, estimated from observations of the dense outflow from Storfjord, Svalbard into the Norwegian Sea, one of the few observed cases of slope convection in the Arctic, a volume increase due to entrainment of around 500% [Backhaus et al., 1997]. The final outflow density is therefore considerably more sensitive to variations in the density of the ambient water.

These results indicate that the mixing with the ambient oceanic waters and its properties, are of considerable importance in determining the properties of the product water and thus the depth of t 0 10.98 509.128

Many dense bottom outflows entrain a number of different ambient water masses during their descent, leading to distinct product water characteristics. For instance, the ambient waters entrained by the dense outflow from Storfjord, Svalbard include East Spitsbergen shelf water, Atlantic water and Norwegian Sea deep water [Quadfasel et al., 1988; Schauer, 1995]. Realistic simulations of overflows must therefore incorporate the density properties of a number of overlying water masses and their mixing accurately.

Entrainment of overlying seawater during the descent of dense bottom flows has a number of important roles in their downslope propagation. Without entrainment, the downslope propagation of down slope front (of the dense outflow) is severely constrained by friction. Friction restricts the supply of dense water from the flow behind to the downslope front, which is needed to force density-driven propagation of the outflow. Turbulent entrainment thickens the downslope front, allowing a greater supply of dense water to the downslope front and so increasing the downslope speed of the outflow [Shapiro et al., 2003]. Also, the entraining outflow transfers ambient water mass properties to depth. For example, a cold and saline plume entraining warm and saltier ambient waters may achieve a net downward transport of heat and salt in the ocean waters [Ivanov et al., 2004; Backhaus et al., 1997]. This is in contrast to open ocean convection, which usually accounts for an upward transport of heat and salt, as occurs in the Greenland Sea for example [Rudels and Quadfasel, 1991].

3.9. Detrainment and the ambient water

The overflow generally descends through a stably stratified oceanic environment. Numerical models of overflows demonstrate the important effect of ambient stratification on the propagation of the outflow. The density contrast between the overflow and the stratified ambient water decreases with depth, as the density of the stratified water increases with depth. Jiang and Garwood [1998] found that as well as this direct effect, in a stratified environment the density contrast further decreases due to enhanced mixing. The descent of an overflow is therefore impeded by ambient stratification and as such the down slope penetration is greater for weak stratification. High latitude outflows are therefore more likely to reach the bottom as the oceanic water column in polar and subpolar seas is typically weakly stratified, such as in Weddell Sea [Price, 1994].

Laboratory experiments [e.g. Lane-Serff and Baines, 1998] show that in a stratified environment such as that of the ocean, and for sufficiently shallow slope angles comparable with those of the continental slope, fluid detrains from the dense plume over most of its length. These experiments were conducted in non-

rotating environments. However, their existence in the ocean is implied by observations, and other experiments show that the effects are also present in rotating fluids, although they remain to be quantified.

Fluid nearer the density front of the overflow is not fully mixed with fluid closer to the bottom and small-scale turbulent mixing processes at the density front [Baines and Condie, 1998], or possibly strong changes in direction of the flow due to local bathymetry [Lane-Serff, 2001], may cause some of this fluid to leave the main plume [Baines and Condie, 1998]. Any mixed fluid formed at the density front in a homogenous environment is still denser than the ambient water and therefore eventually rejoins the dense bottom flow. With a stratified environment, the density of the mixed fluid may equal that of the ambient water at shallower depths than the final depth reached by the main flow. The mixed fluid may thus be shed from the overflow at its own density level [Lane-Serff, 2001] and some dense shelf or marginal sea water therefore enters the ambient ocean over a broad range of depths [Baines and Condie, 1998]. The detrained fluid may form eddies [Etling et al., 2000] or domes of rotating dense water [Lane-Serff, 2001]. Relatively well mixed domes of fluid have been observed downstream of the Mediterranean Sea outflow, which propagate around the North Atlantic for substantial amounts of time.

3.10. Sediment

Model investigations on the influence of suspended sediments in bottom gravity flows indicate their possibly significant role in enhancing cascading and hence water mass formation [Backhaus et al., 1997]. This is substantiated by geological data [Fohrmann, 1996 in Backhaus et al., 1997]. Sediments may be initially dispersed in sufficiently strong bottom gravity flows, or eroded during its descent thereby increasing the density of the flow due to the extra weight of suspended particles [Backhaus et al., 1997 and Baines and Condie, 1998]. The flow forms a turbidity current with suspended sediments increasing the density and therefore the negative buoyancy of the bottom gravity plum

the ambient ocean. The final depth of a sediment-laden outflow is not therefore necessarily dependent on its enhanced density due to the suspended sediments.

Figure 3.3. Schematic of the isopycnal intrusion of a sediment-laden gravity plume from sloping topography. Settling of sediments causes upward directed internal convection [reproduced from Backhaus et al., 1997].

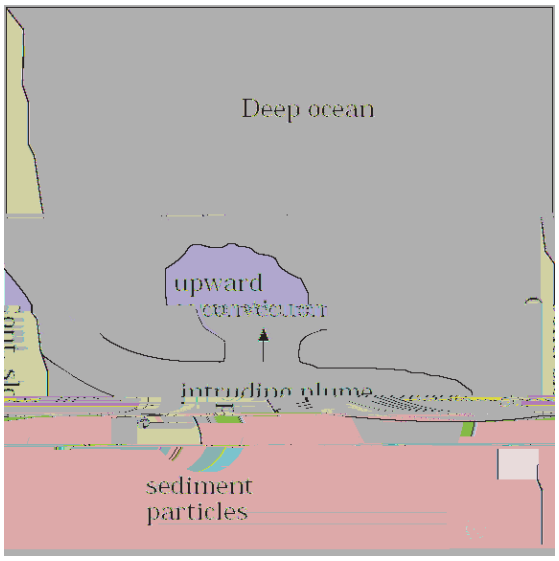

Sediment deposition at the base and lower areas of the continental slope, such as th

initial source water properties and crucially on the properties of ambient water and the amount that is entrained into the overflow, as already discussed in this chapter. The descended water detaches from the continental slope at its equilibrium density level and spreads isopycnally into the ambient waters of the deep ocean. This intrusion may be at intermediate or deep levels, or if the density excess of the cascading flow remains at the foot of the slope, the descended dense water may spread over the ocean floor and become the b

Chapter 4

Simple Plume Model

4.1. Introduction

In order to realistically reproduce overflow dynamics, it is necessary to account for all major processes involved. However, much simpler models allow us to isolate and gain insight into the underlying physical mechanisms. A simplified *process* model is useful for analysing outflow dynamics and for examining specific cascading mechanisms. For example, a process model can be used to estimate the sensitivity of the outflows t

where h is the vertical thickness of the dense layer and H is the depth of the topography from the sea surface. Within this layer the density has a uniform value $\rho_0 + \Delta\rho$, where ρ_0 is the density of the unstratified ambient fluid. F ETent fluid.

The equations of motion for this model are therefore the momentum

where

$$\underline{u}_c = \frac{rg'}{f^2}\nabla H - \frac{g'}{f}\underline{k}\times\nabla H = \frac{rg'}{f^2}\frac{\partial H}{\partial x} + \frac{g'}{f}\frac{\partial H}{\partial y}, \frac{rg'}{f^2}\frac{\partial H}{\partial y} - \frac{g'}{f}\frac{\partial H}{\partial x}$$

is the characteristic velocity. The *x*-axis is directed horizontally eastwards, the *y*-axis is directed northwards alongslope and the *z*-axis is directed upwards as indicated in Figure 4.1. For $r << f$ the characteristic velocity is directed at an approximately fixed angle to the bathymetric contours where the angle of descent is $\frac{r}{f}$. The second term on the right hand side of (5) is diffusive, but generally small.

Assuming the width of the current is far less than the characteristic length scale along the current, (5) can be approximated by

♦

Note, the second term on the right hand side is not written in conservative form and a forward step discretisation is not an optimal choice. Given more time, a range of schemes would have been investigated, such as Runge-Kutta. In addition, although the scheme is numerically convergent, comprehensive convergence testing has not been undertaken due to time restrictions.

4.5. Boundary conditions

The initial condition of the outflow is a parabola with an approximate width, w_0, of 50 km and thickness at the vertex, h_0, of 150 m as indicated in Figure 4.2. Marginal sea outflows are thin, having aspect ratios in the range 0.001 < depth/width < 0.01 [Price, 1994] and the initial condition is based on the values used in Price and Baringer [1994] to model the Denmark Strait Overflow. The exact value used is altered slightly depending on the bathymetry in order to preserve the initial area of the outflow. The flow is started at time *t*

4.6. Choice of bathymetry

A number of forms of bathymetry are considered in order to investigate the effect of steep slope regions on the descent of a dense plume.

(a) Constant slope

In the first numerical experiment, the bottom topography is represented by a plane as illustrated in Figure 4.3, where

$$\frac{dH}{dx} = \tan\theta ,$$

$$\frac{dH}{dy} = 0$$

and $\nabla^2 H = 0$.

(b) Concave slope

A parabola about the constant slope represents the concave bottom topography, as illustrated in Figure 4.4. The topography varies only in the *x* direction and hence

$$\frac{dH}{dy} = 0 .$$

The height and width of the bathymetry parabola are given similarly to the initial condition of the outflow as illustrated in Figure 4.2. The height is the perpendicular distance of the vertex from the constant slope, and the width is the distance, parallel to the constant slope, between where the parabola intersects the constant slope.

(c) Convex slope

A parabola about the constant slope represents the convex bottom topography, as illustrated in Figure 4.5. The topography varies only in the *x* direction and hence

$$\frac{dH}{dy} = 0 .$$

The height and width of the bathymetry parabola are given similarly to the concave bathymetry.

(d) Corrugated slope

A corrugation (oscillation) of the bottom topography in the *y* direction around the constant slope, as illustrated in Figure 4.6, is represented by the addition of a second term on the right hand side.

$$\frac{dH}{dx} = \tan\theta + a\sin(ky)$$

and $$\frac{d^2H}{dx^2} = 0$$

where *a* is the amplitude of the corrugation and *k* is the period. Integrating we obtain

$$H = x\tan\theta + ax\sin(ky) + \mathrm{H}_0$$

Therefore

$$\frac{dH}{dy} = akx\cos(ky)$$

$$\frac{d^2H}{dy^2} = -ak^2x\sin(ky)\,.$$

Figure 4.4. The model concave slope bathymetry. The bathymetry shown is calculated along 59 characteristics in total, where characteristics 11 to 49 capture the initial outflow. The left and right edges of the shaded region follow characteristics 1 and 59. The remaining characteristics are between these and converge with increasing *y* although this is not clearly visible in this case. The colour scale is the depth in metres below H

The bathymetry shown is
pture the initial outflow.
e remaining characteri
ible in this case. Th

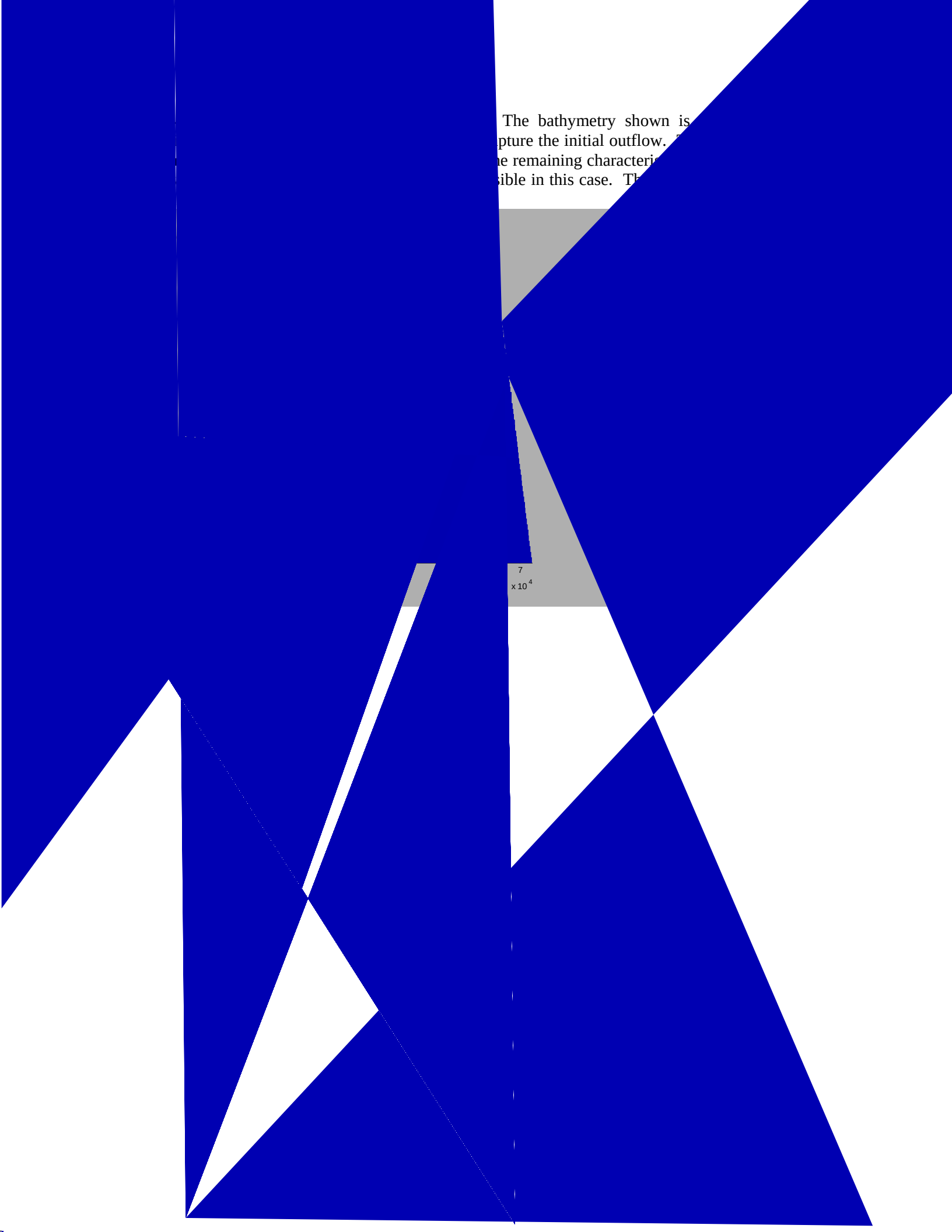

Figure 4.6. The model corrugated slope bathymetry. The bathymetry shown is calculated along 59 characteristics in total, where characteristics 11 to 49 capture the initial outflow. The left and right edges of the shaded region follow characteristics 1 and 59, with the remaining characteristics between these. The colour scale is the depth in metres below H_0. The amplitude, a, of the corrugation is given as a function of

4.7. Results: Path of the flow

Once initialised, only the characteristic velocity and therefore the bottom topography determine the path of the flow along the characteristics. In this section we examine and compare the rates of descent along the characteristics for each of the four different bottom topographies. Although outflows can flow for hundreds of kilometres downstream, the cross slope angle in large outflows is quite small. For the convex and concave cases the topography varies only in the across stream (x) direction. In order to emphasize any effects of the topography, the friction is taken to be the slightly inflated value of 5×10^{-6} s^{-1} in order to increase the cross slope angle, and the model is allowe

takes longer to descend. This is most likely due to the overall greater distance travelled over the curved bathymetry, which can be inferred from Figures 4.10 and 4.11. The characteristics for corrugated bathymetry converge to those for constant bathymetry as the amplitude of the corrugation decreases, which also decreases the overall distance travelled (Figure 4.10). When the period of the corrugation is halved, this does not affect the overall distance travelled and the time taken does not alter as illustrated in Figure 4.11.

Figure 4.7. The downslope propagation of the characteristics with (a) constant slope bathymetry. (b) concave slope bathymetry. (c) convex slope bathymetry (d) corrugated slope bathymetry. In all cases, the average gradient of the slope is equal to that of the constant slope, tan θ.

(a)

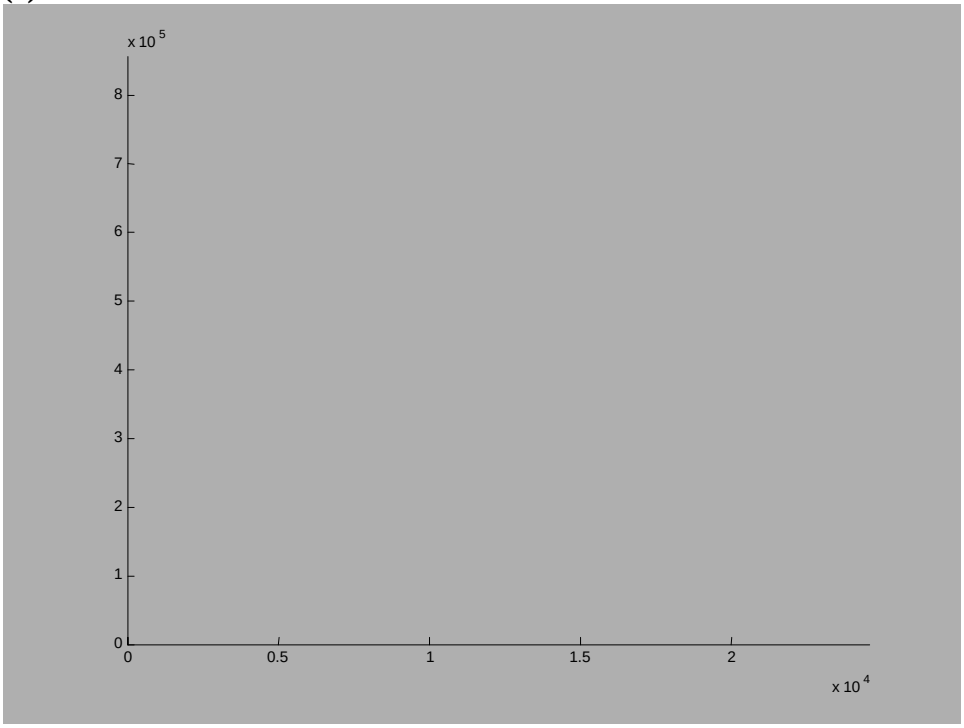

(c)

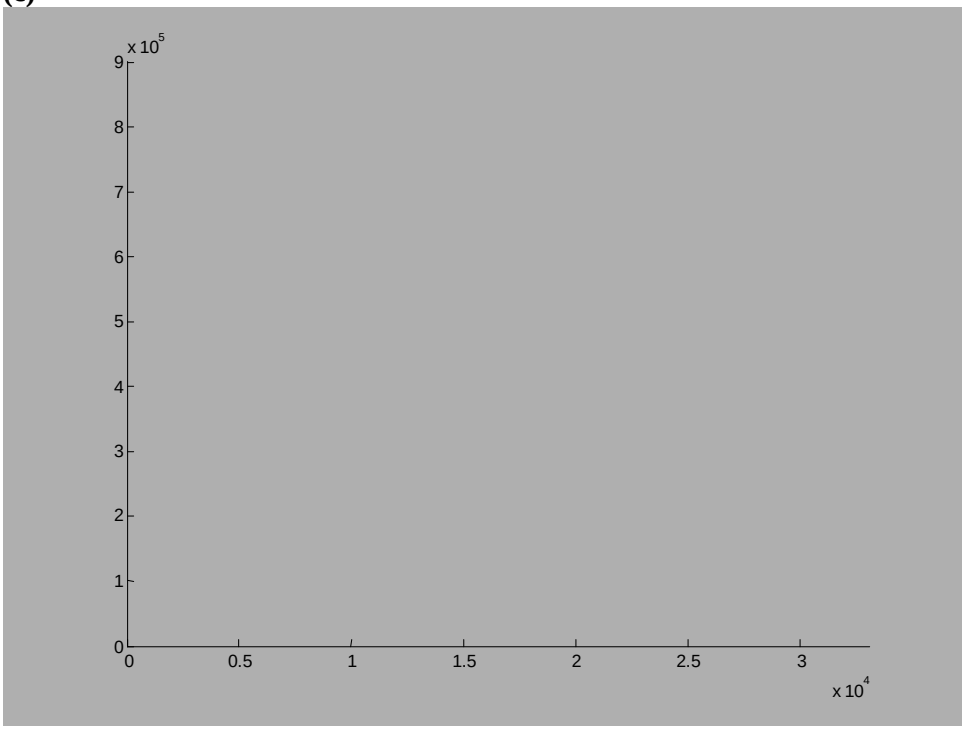

Figure 4.8. The across slope propagation of the characteristics with corrugated slope bathymetry.

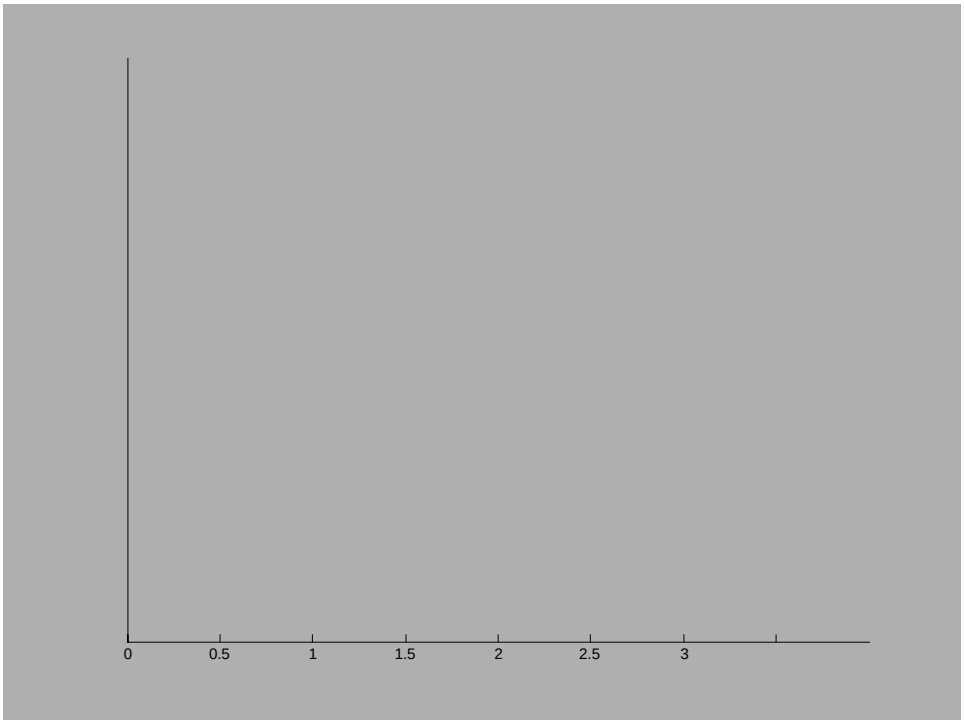

Figure 4.10. Comparison of the times taken along a characteristic to reach a depth level over one period of the corrugation with varying amplitude of the corrugation. The characteristic is initially at $x = y = 0$.

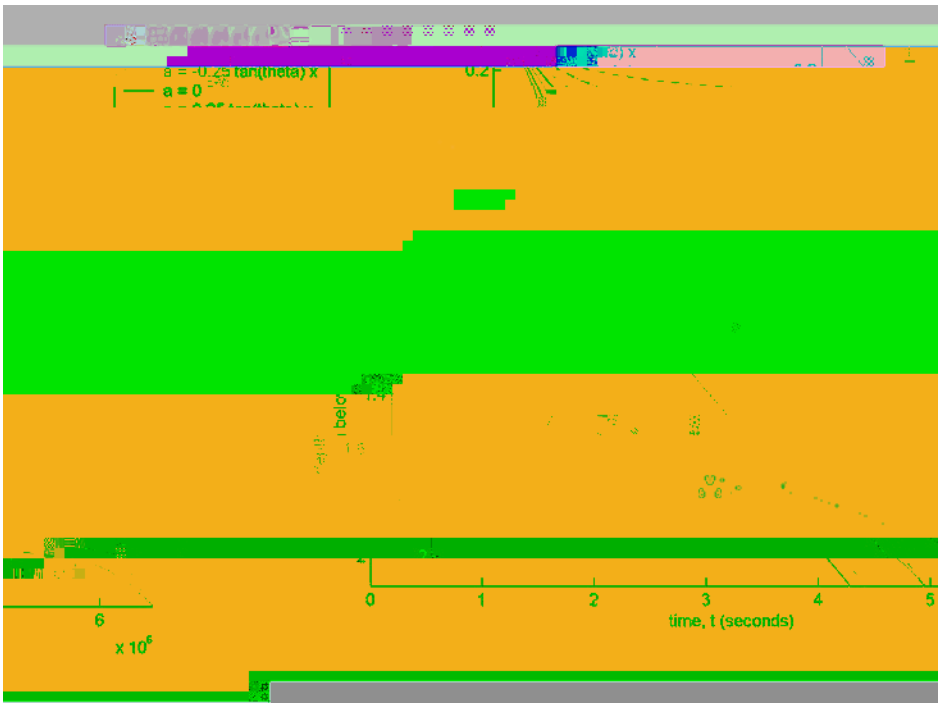

Figure 4.11. Comparison of the times taken along a characteristic to reach a depth level with varying periods of the corrugation. The characteristic is in

4.8. Results: Evolution of the flow

In this section, we use the numerical scheme given by (8) to calculate the evolution of the vertical thickness of the dense overflow along the characteristics and analyse the effects of topography. The flow is calculated along 59 characteristics in total, with characteristics 11 to 49 capturing the initial outflow. The extra characteristics allow for diffusive spreading of the flow. The drag coefficient, $r = 5 \times 10^{-6}$ s^{-1} and the model is run until $y = -10^6$, which is more realistic than the value used in Section 4.4.

Figures 4.12.(a)-(d) shows the flattening of the overflow water as it diffuses and spreads over the ocean floor in each case and this is highlighted in Figure

Figure 4.12. The along slope evolution of the thickness of the dense overflow along the characteristics with (a) constant slope bathymetry. (b) concave slope bathymetry. (c) convex slope bathymetry. (d) corrugated slope bathymetry.

(b)

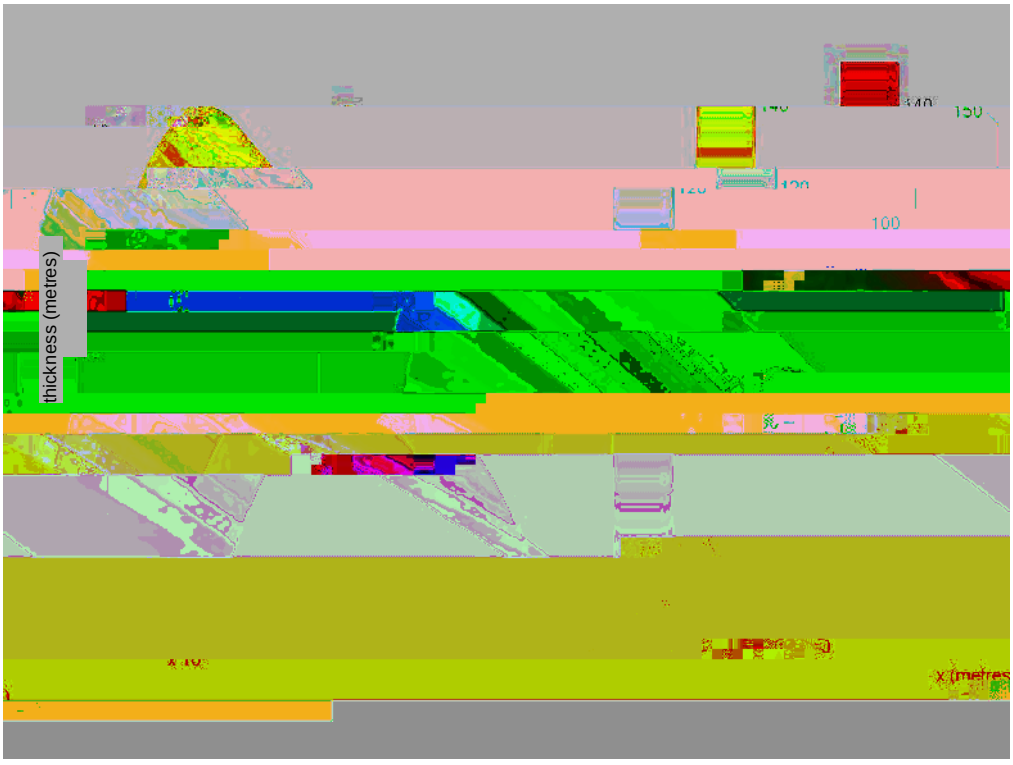

(c)

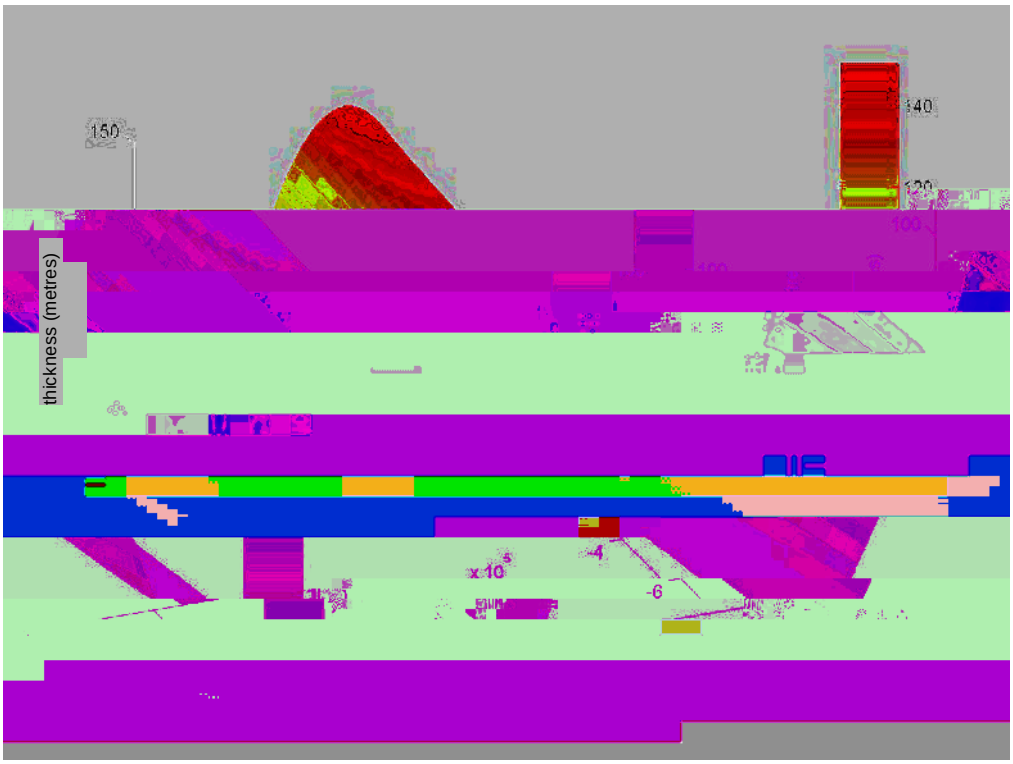

(d)

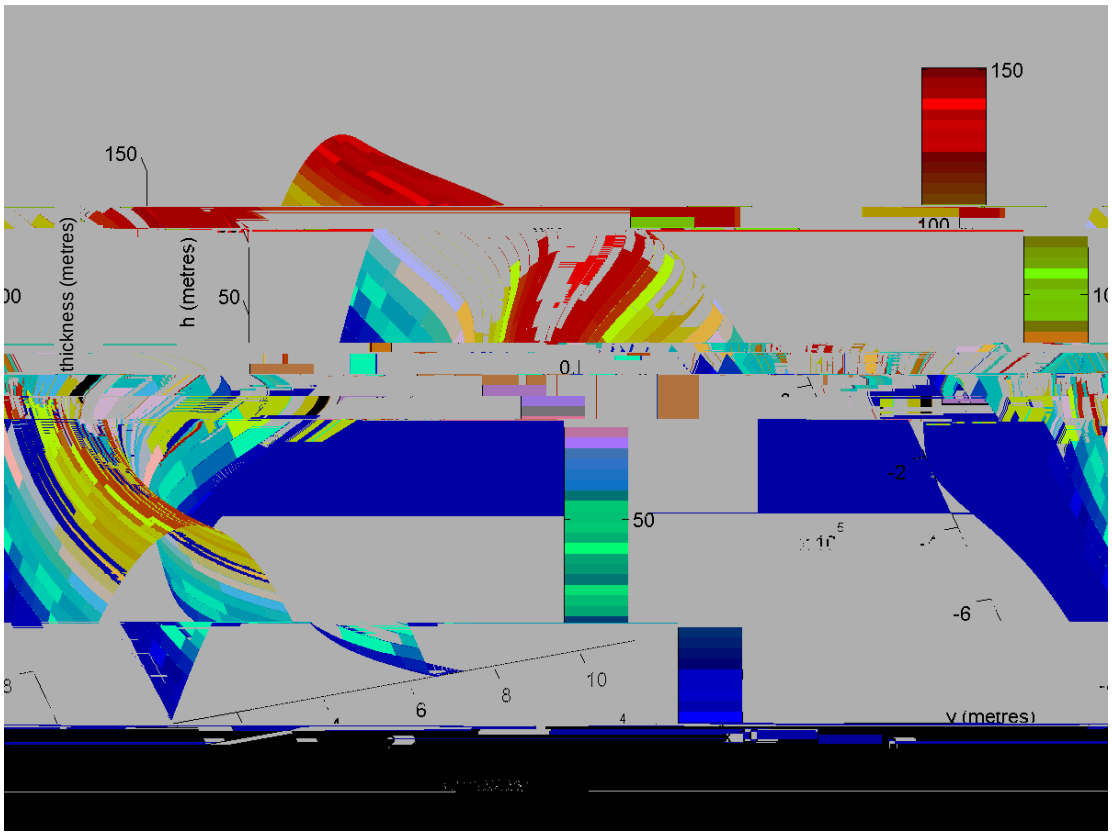

Ekman drainage provides a larger component to the downslope flow. A weak source is viscously controlled and the only transport is drainage in the Ekman layer.

In addition, topography can alter the dynamical balance and features such as canyons may steer the dense flow rapidly downslope, or a topographic saddle point may possibly split the flow. Real topography on a scale comparable to topographic features that may aff

circulation. The role of slope convention in maintaining essential exports of gasses, nutrients and pollutants etc. from productive shelf regions to the deep ocean is not considered in this study. It is likely to be highly important although current models of biogeochemical cycles cannot account for overflow

Due to time constraints, there remain many improvements to be made to the model and a large amount still to be investigated. The numerical scheme could be improved using a full conservative form and, for example, a Runge-Kutta scheme. Comprehensive convergence testing also needs to be completed. More realistic bottom drag can easily be incorporated using a quadratic friction term. Entrainment of overlying lighter water could also be added and the effects investigated. Although beyond the scope of the present study, real bottom topography, and oceanic temperature and salinity profiles, could be incorporated.

Notation

h	Vertical thickness of the dense layer	m
H	Depth of the topography from the sea surface	m
H_0	Horizontal datum level	m
ρ_0	Density of the unstratified ambient fluid	

Notation Density
m bient fluid

m 0

Acknowledgements

I would like to thank Professor David Marshall for his help, contribution and time. Thanks also to Owen, my course mates, and the financial support received from NERC that enabled me to complete this course.

References

Backhaus, J.O., Fohrmann, H., Kämpf, J. and Rubino, A. (1997) ‘Formation and export of water masses produced in Arctic shelf polynyas – process studies of oceanic Convection’, (,) T j / T T 1 1 T f 0 2 2

stu,(n)Tj10.98 0 0 10.98 187580.92 239.56998 T S, A. (199 99ArctDownslope Flows: Aer

y

Killworth, P.D. (2001) ‘On the rate of descent of overflows’,

Wunsch, C. and Ferrari, R. (2004) ‘Vertical mixing, energy and the general circulation of the oceans’, *Annual Review of Fluid Mechanics*, 36, 281-314.

Zoccolotti, L., and Salusti, E. (1987) ‘Observations of a vein of very dense marine water in the southern Adriatic Sea’ *Continental Shelf Research*, 7**,** 535–551.